

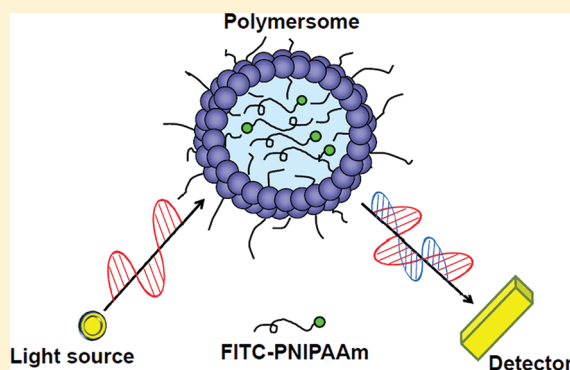
# Time-Resolved Fluorescence and Fluorescence Anisotropy of Fluorescein-Labeled Poly(*N*-isopropylacrylamide) Incorporated in Polymersomes

Jung Seok Lee,<sup>†</sup> Rob B. M. Koehorst,<sup>‡,§</sup> Herbert van Amerongen,<sup>‡,§</sup> and Jan Feijen<sup>\*,†</sup>

<sup>†</sup>Department of Polymer Chemistry and Biomaterials, Institute for Biomedical Technology and Technical Medicine, MIRA, Faculty of Science and Technology, University of Twente, P.O. Box 217, 7500 AE, Enschede, The Netherlands

<sup>‡</sup>Laboratory of Biophysics, and <sup>§</sup>MicroSpectroscopy Centre, Wageningen University, Wageningen, The Netherlands

**ABSTRACT:** The phase behavior of fluorescein isothiocyanate (FITC) labeled poly(*N*-isopropylacrylamide) (PNIPAAm) incorporated in polymersomes (Ps) was studied by monitoring the fluorescence lifetime (FL) and the time-resolved fluorescence anisotropy (TRFA) as a function of temperature at pH 7.4. Ps containing FITC-labeled PNIPAAm with a diameter less than 200 nm were prepared by injecting a THF solution of poly(ethylene glycol)-*b*-poly(*D,L*-lactide) (mPEG-PDLLA) and FITC tagged PNIPAAm (FITC-N) into phosphate buffered saline (PBS, pH 7.4). Solutions of free FITC (2  $\mu$ M) and FITC-N (2  $\mu$ M) in PBS were used as controls. The polarized fluorescence decay curves of FITC were fitted with one rotational correlation time ( $\theta_1$ ) and the corresponding amplitude ( $\beta_1$ ), while those for FITC-N were fitted with two rotational correlation times ( $\theta_{1,2}$ ) and their corresponding amplitudes ( $\beta_{1,2}$ ). Short rotational correlation times,  $\theta_1$ , correspond with the rotation of the FITC molecule itself, whereas  $\theta_2$  corresponds to FITC-segmental rotation. FITC-N encapsulated in Ps (FITC-N/Ps) showed a decrease of the rotational motion upon increasing the temperature. The long rotational correlation time ( $\theta_2$ ) of FITC-N increased 3 fold, going from 15 to 40  $^\circ$ C, reflecting a reduced rotational mobility. The residual anisotropy ( $\beta_\infty$ ) of FITC-N/Ps at pH 7.4 showed a gradual increase, going from 15 to 25  $^\circ$ C followed by a gradual decrease at higher temperatures. These results are explained by a transition from coil to globule, a gradual increase of intermolecular aggregation, and possibly phase separation and hydrogel formation.



## INTRODUCTION

Polymersomes (Ps), synthetic supramolecular structures similar to liposomes but composed of amphiphilic block copolymers instead of lipids,<sup>1</sup> have attracted a lot of attention for drug delivery applications due to their outstanding stability and relatively long residence times in the circulation.<sup>2,3</sup> Significant efforts have been devoted to control drug delivery from Ps by varying the length and composition of the consisting block copolymers, by using block copolymers that are temperature sensitive, pH-responsive, or that are chemically or physically cross-linked.<sup>4,5</sup> An alternative approach is to modify the interior of the Ps for instance by the introduction of a hydrogel. Poly(*N*-isopropylacrylamide) (PNIPAAm) may be used as a precursor of a thermo-sensitive hydrogel. PNIPAAm dissolved in water shows temperature-induced dehydration of the polymer chains, which can be followed by the formation of a hydrogel depending on the molecular weight of the PNIPAAm and the concentration of the PNIPAAm solution.<sup>6</sup> Above the lower critical solution temperature (LCST) of the PNIPAAm solution, aggregation of the PNIPAAm polymer chains takes place by intermolecular hydrophobic interaction, leading to phase separation into an aqueous

phase and a hydrogel.<sup>7</sup> This behavior of PNIPAAm has been used to form a hydrogel either in liposomes or in Ps.<sup>8,9</sup>

In recent years, tracking of the photophysical properties of a molecular probe by fluorescence spectroscopy has become a versatile technique to detect changes in the local environment of the probe. Fluorescently labeled compounds located in a heterogeneous environment can be followed in time by using time-resolved fluorescence techniques. These techniques have been used for better understanding of protein–substrate, protein–receptor, and lipid–protein interactions as well as for probing the local environment of a dye in micelles or liposomes<sup>10,11</sup> and to characterize sol–gel transitions.<sup>12</sup> It has also been reported that a sol–gel transition of PNIPAAm to form microgels and the sol–gel transition to form a silica gel matrix could be followed by fluorescence analysis.<sup>13–15</sup> On the basis of these findings, we assume that a time-resolved fluorescence study may also

Received: July 25, 2011

Revised: October 12, 2011

Published: October 13, 2011

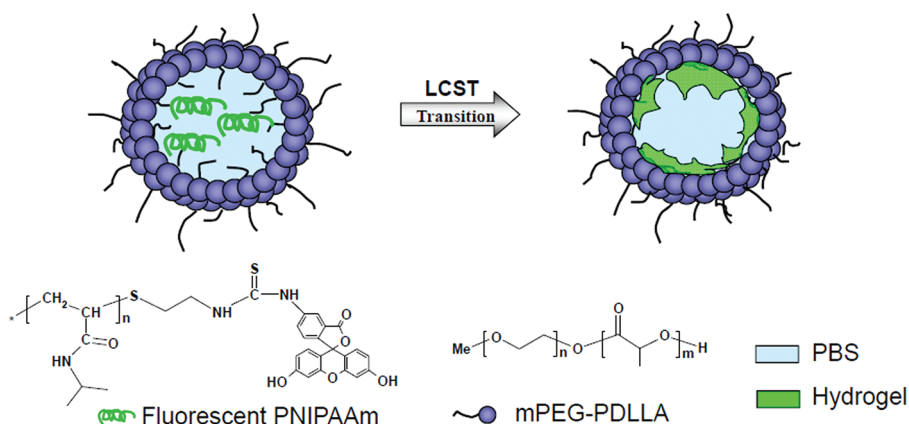


**Figure 1.** Schematic 2D-cross sectional illustration of FITC-N/Ps. At the LCST, phase separation of the FITC-N solution present in the core of Ps into an aqueous phase and a hydrogel takes place.

allow us to characterize the temperature-dependent formation of a PNIPAAm hydrogel inside Ps.

In principle, this can be achieved by incorporation of a fluorescent dye labeled PNIPAAm into the Ps. Fluorescence anisotropy and fluorescence lifetime studies of this labeled PNIPAAm may give information about temperature-induced changes in the interior of the Ps. Fluorescein isothiocyanate (FITC), a derivative of fluorescein that can be easily reacted with amine groups, was selected as a fluorophore to label PNIPAAm because of its high quantum yield and adequate photostability. The fluorescent properties of FITC derivatives are strongly affected by the environment.<sup>16</sup> Therefore, it will be very useful for monitoring physical parameters like local mobility of the environment and rotational dynamics of labeled PNIPAAm in Ps.

The aim of this work is to investigate the thermo-responsive behavior of FITC-labeled PNIPAAm (FITC-N) in Ps by measuring the time-resolved fluorescence anisotropy (TRFA) and fluorescence lifetime profiles (FL). For this study, FITC was first coupled to PNIPAAm (FITC-N) and then incorporated into Ps by injecting a THF solution of the Ps forming polymer and FITC-N into PBS (pH 7.4). Poly(ethylene glycol)-*b*-poly(D,L-lactide), mPEG-PDLLA, was used as a biodegradable and biocompatible amphiphilic block copolymer for the formation of the Ps. A schematic picture of Ps containing a FITC labeled hydrogel and the chemical structure of the polymers used for the system is given in Figure 1. TRFA and FL of FITC-N in Ps were measured as a function of temperature, and the results were compared to those for the corresponding free solutions of FITC and FITC-N.

## EXPERIMENTAL METHODS

**Materials.** D,L-Lactide (DLLA, Purac Biochem b.v., The Netherlands), *N*-isopropylacrylamide (NIPAAm, Aldrich, U.S.), and 2,2'-azobisisobutyronitrile (AIBN, Fluka, Switzerland) were recrystallized from toluene, hexane, and methanol, respectively. Monomethoxy poly(ethylene glycol) with a molecular weight of 5000 g/mol (mPEG, Iris Biotech, Germany) was dried by dissolution in anhydrous toluene followed by azeotropic distillation under N<sub>2</sub>. Stannous octoate, Sn(Oct)<sub>2</sub>, was obtained from Sigma (U.S.). Fluorescein isothiocyanate (FITC) and 2-aminoethanethiol (AET) were purchased from Fluka (Switzerland) and used as received. Phosphate buffered saline (PBS, 0.01 M, pH 7.4, B. Braun, U.S.) was used as a medium for the FL and TRFA experiments.

**Synthesis of Polymers and Preparation of FITC-Labeled PNIPAAm-Containing Ps.** mPEG-PDLLA and FITC-labeled PNIPAAm (FITC-N) were prepared as previously reported.<sup>8</sup> mPEG-PDLLA was synthesized by ring-opening polymerization (ROP) of DLLA using mPEG as an initiator. Amino terminated PNIPAAm was synthesized by free radical polymerization of NIPAAm using AET as a chain transfer agent, and the resulting polymer was reacted with FITC. <sup>1</sup>H NMR analysis (Inova 300 MHz, Varian, U.S.) showed that the monomer conversion of DLLA was 99% and the *M<sub>n</sub>* of the PDLLA block was 42 000 g/mol. *M<sub>n</sub>* and *M<sub>w</sub>* of PNIPAAm were analyzed by gel permeation chromatography (GPC) as 39 200 and 56 000 g/mol, respectively. The labeling efficiency of PNIPAAm with FITC was determined by fluorescence spectroscopy using FITC-dextran (Fluka, 40 000 g/mol) as a standard.

Polymersomes with encapsulated FITC-N, FITC-N/Ps, were prepared using the solvent injection method. In brief, mPEG-PDLLA (10 mg/mL) and FITC-labeled PNIPAAm (FITC-N, 50 mg/mL) were dissolved in THF (1 mL), and the resulting solution was injected into PBS (50 mL). After 15 min without shaking, the vial containing the mixture was turned upside down several times, resulting in a turbid dispersion. THF was removed by dialysis using a dialysis membrane (cutoff 50 000 g/mol, Spectra/Por, CA) in PBS for 2 days, and subsequently nonencapsulated FITC-N was removed by ultrafiltration through a membrane (cutoff 100 000 g/mol, Ultracel Ultrafiltration Disc, Millipore, U.S.) for 5 h.

**Data Acquisition.** Time-resolved polarized fluorescence experiments were carried out using the time-correlated single-photon counting technique (TCSPC).<sup>17</sup> The TCSPC setup and the measurement procedures used were described in detail elsewhere<sup>18</sup> and will only briefly be outlined below. Samples, placed in a static cuvette holder, temperature controlled by applying thermoelectric (Peltier) elements and a controller (Marlow Industries Inc., Dallas, TX, model SE 5020), were excited with vertically polarized 470 nm pulses of around 0.2 ps duration at a repetition rate of 3.8 MHz. Measurements were done by collecting repeated sequences of 10 s vertically (parallel) and 10 s horizontal (perpendicular) polarized fluorescence emission. Fluorescence was detected using a Schott OG515 nm cutoff filter in combination with a Balzers K55 broadband interference filter (550 nm).

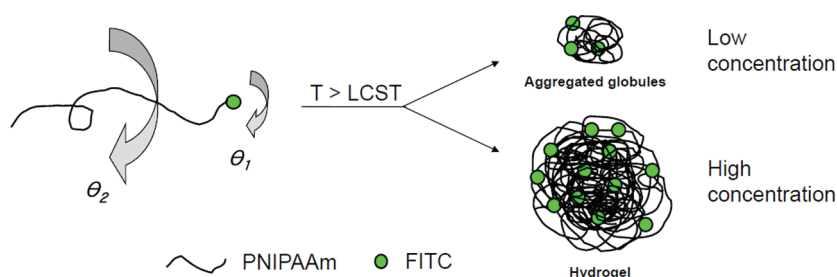


**Figure 2.** Schematic illustration of possible positions of FITC linked to PNIPAAm in the solution or incorporated in the PNIPAAm gel. PNIPAAm exhibits a coil to globule transition by increasing the temperature due to dehydration of the polymer chains. Depending on the molecular weight of PNIPAAm and the concentration of the polymer solution, the coil to globule transition can be followed by phase separation into a hydrogel and an aqueous phase (inside Ps). FITC will be associated either with the globular state of PNIPAAm or with the gel formed in the Ps at higher temperatures. A short rotational correlation time,  $\theta_1$ , and a long rotational correlation time,  $\theta_2$ , are presented.  $\theta_1$  relates to the rotation of individual FITC molecules, whereas  $\theta_2$  is related to the rotation of FITC in conjunction with PNIPAAm segments.

The data were collected using a multichannel analyzer with a maximum time window of 4096 channels typically at 5 ps/channel. The dynamic instrumental response function of the setup was approximately 40–50 ps fwhm and was obtained at the FITC emission wavelength using a solution of erythrosine B in deionized water as reference compound ( $\tau_{\text{ref}} = 80$  ps). Although this lifetime is relatively long as compared to the 40–50 ps fwhm, it is significantly faster than the observed kinetics in the rest of this study, and the analysis software can correctly account for this lifetime in the overall fitting process. One complete experiment for a fluorescence decay measurement consisted of the recording of data sets of the reference compound, the FITC samples, the background (buffer), and again the reference compound.

**Data Analysis.** Data analysis was performed using a model of discrete exponential terms.<sup>19</sup> Global analysis of the experimental data was performed using the “TRFA Data Processing Package” of the Scientific Software Technologies Center (Belarusian State University, Minsk, Belarus).<sup>20,21</sup> The isotropic fluorescence intensity decay  $F_{\text{iso}}(t)$  was obtained from the measured decay curves of parallelly  $F_{\parallel}(t)$  and perpendicularly  $F_{\perp}(t)$  polarized emission:

$$F_{\text{iso}}(t) = F_{\parallel}(t) + 2gF_{\perp}(t) \quad (1)$$

using the relative sensitivity  $g$  of the detection branch for parallelly and perpendicularly polarized light ( $g$  equals unity for this setup<sup>22</sup>).

$F_{\text{iso}}(t)$  was fitted to a sum of exponentials with lifetime  $\tau_i$  and amplitude  $\alpha_i$ , convoluted with the instrument response function, IRF, according to eq 2, where  $E(t)$  is the IRF.<sup>20</sup>

$$F_{\text{iso}}(t) = E(t) \otimes \sum_{i=1}^N \alpha_i e^{-t/\tau_i} \quad (2)$$

The quality of the fit was judged by the  $\chi^2$  value (below 1.1 was considered sufficient) and by the quality of the residuals and autocorrelation of these residuals. Average fluorescence lifetimes,  $\tau_{\text{av}}$ , were calculated according to eq 3.<sup>23</sup>

$$\tau_{\text{av}} = \frac{\sum_{i=1}^N \alpha_i \tau_i^2}{\sum_{i=1}^N \alpha_i \tau_i} \quad (3)$$

The anisotropy decay  $r(t)$  is given by the following relation:

$$r(t) = \frac{F_{\parallel}(t) - F_{\perp}(t)}{F_{\parallel}(t) + 2gF_{\perp}(t)} \quad (4)$$

In fluorescence anisotropy analysis, after deconvolution, the time-dependent fluorescence anisotropy  $r(t)$  is analyzed by global fitting of  $F_{\parallel}(t)$  and  $F_{\perp}(t)$ , with fit parameters  $\tau_j$  (fluorescence lifetimes),  $\alpha_j$  (fluorescence decay amplitudes),  $\theta_j$  (anisotropy correlation times),  $\beta_j$  (anisotropy amplitudes), and  $\beta_{\text{inf}}$  (residual anisotropy), using fit functions:

$$F_{\parallel}(t) = \frac{1}{3} \sum_{i=1}^N \alpha_i e^{-t/\tau_i} \{1 + 2(\beta_{\infty} + \sum_{j=1}^M \beta_j e^{-t/\theta_j})\} \quad (5)$$

and

$$F_{\perp}(t) = \frac{1}{3} \sum_{i=1}^N \alpha_i e^{-t/\tau_i} \{1 - (\beta_{\infty} + \sum_{j=1}^M \beta_j e^{-t/\theta_j})\} \quad (6)$$

in which  $i = j$  for correlated systems in which particular lifetime components  $\tau_i$  are associated with particular correlation times  $\theta_j$  (correlated or associative model), and  $i \neq j$  for systems in which all lifetimes equally contribute to the anisotropy (uncorrelated or nonassociative model). Because the associative method did not lead to clear correlations between fluorescence lifetimes and rotational correlations times, the latter method (nonassociative model) was used for the fitting in this study.

## RESULTS AND DISCUSSION

Ps containing FITC-N, FITC-N/Ps, with a diameter less than 200 nm were prepared and characterized as previously reported.<sup>8</sup> The degree of functionalization of PNIPAAm with amine groups was  $96.0 \pm 4.7$  mol %, and the labeling efficiency of PNIPAAm-NH<sub>2</sub> with FITC was  $94.0 \pm 11.8$  mol %. To acquire the internal dynamics of the label bound to PNIPAAm in Ps, FL profiles and TRFA of FITC-N in Ps were measured. Solutions of free FITC (2  $\mu\text{M}$ ) and FITC-N (2  $\mu\text{M}$ ) in PBS were used for comparison.

To explain the FL and TRFA data that will be discussed later, first a model (Figure 2) is presented that shows the possible temperature-dependent changes in the local environment of the fluorescent probes. PNIPAAm in solution at relatively low concentrations exhibits a temperature-induced coil to globule transition due to dehydration of the polymer chains. Depending on the molecular weight of PNIPAAm and at sufficiently high concentrations of the polymer solution, like in the Ps, the coil to



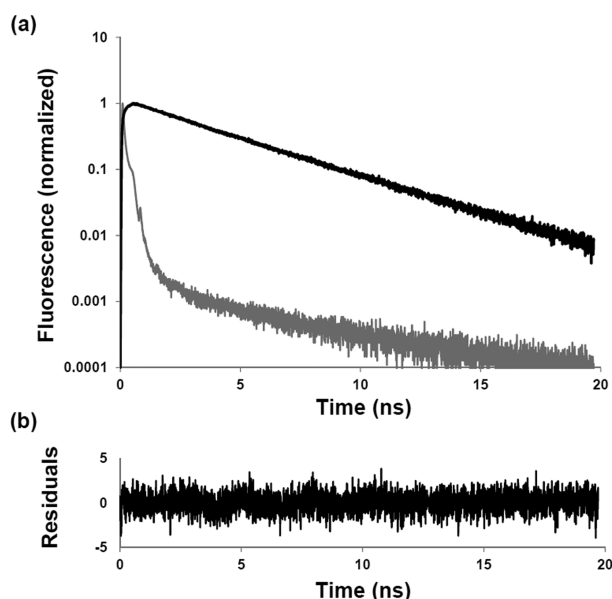


**Figure 3.** A fluorescence decay curve for FITC-N in PBS at 25 °C. Normalized fluorescence decay (black) and the “instrument response function” (“IRF”, gray) are represented in (a). The residuals of a three-exponential fit are shown in (b). Note that for illustration purposes the “IRF” in this case is a convolution of the real IRF with the fluorescence decay of pinacyanol, which has a lifetime of 6 ps (for further details, see ref 24).

**Table 1.**  $\tau_{av}^a$  of FITC, FITC-N, and FITC-N/Ps in PBS as a Function of Temperature

	15 °C	20 °C	25 °C	30 °C	35 °C	40 °C
FITC	4.01	3.96	3.92	3.86	3.81	3.74
FITC-N	3.77	3.73	3.72	3.70	3.61	3.46
FITC-N/Ps	3.90	3.96	3.96	4.03	4.01	3.97

<sup>a</sup> Average fluorescence lifetime (ns).

globule transition can be followed by phase separation, leading to the formation of a hydrogel and an aqueous phase. The environment of FITC covalently linked to PNIPAAm will be changed both by the temperature-induced coil to globule transition and by the hydrogel formation after phase separation of PNIPAAm present in the Ps. This may lead to restricted rotational mobility of the probe itself and/or the probe in conjunction with polymer segments. Figure 2 gives a schematic picture of temperature- and concentration-dependent transitions of FITC-labeled PNIPAAm and associated rotational correlation times  $\theta_1$  and  $\theta_2$ .  $\theta_1$  is related to the rotation of individual FITC molecules, whereas  $\theta_2$  is related to the rotation of FITC in conjunction with PNIPAAm segments.

Figure 3 shows a typical example of a fluorescence decay curve for FITC-N in PBS (pH 7.4) at 25 °C and the residuals corresponding to a three-exponential fit. This was also the case for that of buffered solutions (pH 7.4) of free FITC and FITC-labeled PNIPAAm incorporated in polymersomes (FITC-N/Ps), and all fits were of good quality ( $\chi^2 < 1.1$ ).

In Table 1,  $\tau_{av}$  as a function of temperature is shown for a dilute solution of FITC and FITC-N in PBS at pH 7.4 and for FITC-N in polymersomes (FITC-N/Ps). For a solution of free FITC in PBS,  $\tau_{av}$  decreased from 4.01 to 3.74 ns upon increasing

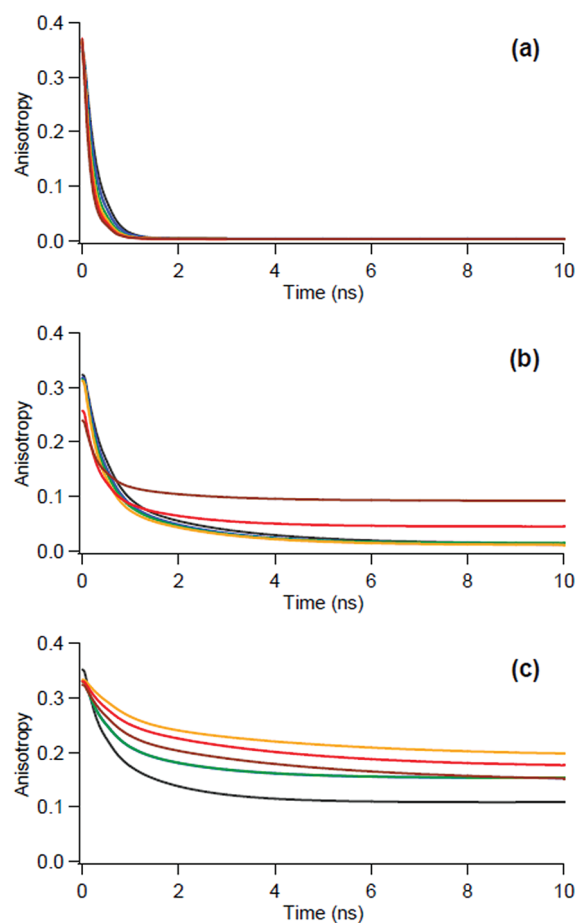


**Figure 4.** Fitted fluorescence anisotropy decay curves of free FITC (a), FITC-N (b), and FITC-N/Ps (c) in PBS at 15 °C (black), 20 °C (blue), 25 °C (green), 30 °C (orange), 35 °C (red), and 40 °C (brown). Time zero was set at the start of the laser pulse (where fluorescence starts to increase) because the software also calculates the anisotropy for the data points before time zero (where there is no fluorescence).

the temperature from 15 to 40 °C, showing a normal temperature effect on fluorescence lifetimes. In general, the lifetimes of excited states are shortened with increasing temperature as a result of an increase of the nonradiative relaxation rate.<sup>25</sup> This was also the case for a dilute solution of FITC-N.  $\tau_{av}$  for the FITC-N solution decreased by increasing the temperature. A coil to globule transition of PNIPAAm may not significantly influence the fluorescence lifetimes of FITC in the dilute solution because FITCs are conjugated at the end of PNIPAAm chains. In contrast,  $\tau_{av}$  of FITC-N in Ps increased upon increasing the temperature up to 30 °C. This may be indicative for the presence of different relaxation patterns of FITC conjugated to PNIPAAm when localized in Ps most probably due to the relatively high concentration of PNIPAAm in the Ps. Above 30 °C, a normal temperature effect on the fluorescence lifetimes of FITC-N in Ps was observed.

The fluorescence anisotropy during the first 10 ns after excitation is presented in Figure 4. In Table 2, the data for rotational correlation times ( $\theta$ ) and their amplitudes ( $\beta$ ) as well as residual anisotropies ( $\beta_\infty$ ) are listed for various temperatures. The short rotational correlation time ( $\theta_1$ ) is related to the rotation of individual FITC molecules, and the long rotational correlation time ( $\theta_2$ ) is associated with the rotation of FITC in conjunction with PNIPAAm segments. The polarized fluorescence decay curves of

**Table 2.** Fluorescence Anisotropy of FITC (2  $\mu$ M), FITC-N (2  $\mu$ M), and FITC-N/Ps in PBS

	temp	$\beta_1^a$	$\theta_1^b$	$\beta_2^a$	$\theta_2^b$	$\beta_\infty^c$
FITC	15 °C	0.36	0.18			0.00
	20 °C	0.36	0.15			0.00
	25 °C	0.37	0.12			0.00
	30 °C	0.37	0.10			0.00
	35 °C	0.37	0.09			0.00
	40 °C	0.37	0.07			0.00
FITC-N	15 °C	0.22	0.27	0.10	2.1	0.01
	20 °C	0.21	0.24	0.09	1.9	0.01
	25 °C	0.21	0.21	0.09	1.6	0.01
	30 °C	0.22	0.19	0.08	1.8	0.01
	35 °C	0.15	0.16	0.06	1.4	0.04
	40 °C	0.11	0.13	0.04	1.2	0.09
FITC-N/Ps	15 °C	0.14	0.20	0.11	1.4	0.11
	20 °C	0.11	0.26	0.08	1.7	0.15
	25 °C	0.06	0.40	0.07	2.8	0.21
	30 °C	0.07	0.45	0.07	3.9	0.19
	35 °C	0.07	0.30	0.09	3.4	0.17
	40 °C	0.09	0.34	0.09	4.2	0.15

<sup>a</sup> Fractional contribution to the fluorescence anisotropy decay. <sup>b</sup> Rotational correlation time (ns). <sup>c</sup> Residual anisotropy.

FITC-N were fitted with two rotational times ( $\theta_{1,2}$ ) and their corresponding amplitudes ( $\beta_{1,2}$ ) using the uncorrelated or non-associative model, in which all lifetimes equally contribute to the anisotropy. The rotational times reflect the local mobility of FITC. In principle, fluorescence depolarization can also be caused by resonance energy transfer<sup>26,27</sup> as will be discussed below.

For free FITC,  $\beta_\infty$  was zero in the temperature range used when fitted with one rotational correlation time ( $\theta_1$ ), which is at most a few hundred picoseconds. The fluorescence anisotropy decay curve of FITC-N shows a relatively low value for  $\beta_\infty$  at the lowest temperatures, which increases upon raising the temperature above 30 °C. The increase of  $\beta_\infty$  with temperature for FITC-N up to 0.09 can be explained by the earlier reported coil-to-globule transition of single PNIPAAm chains at high dilution.<sup>28</sup> The global motion of a globule can be considered as “infinitely slow” with the used time frame of 20 ns, resulting in a residual anisotropy,  $\beta_\infty$ . The contribution of  $\beta_\infty$  to the anisotropy decay increased with raising the temperature above 30 °C (Figure 5a), indicating that a transition occurred at approximately 30 °C. However, rotational correlation times  $\theta_1$  and  $\theta_2$  did not increase during the coil-to-globule transition within the temperature range used. This is probably due to the fact that FITC is bound to the end of the PNIPAAm chains. The slight decrease of  $\theta_1$  and  $\theta_2$  above 30 °C can be considered as a common temperature effect. Alternatively, a coil-to-globule transition might lead to enhanced resonance energy transfer and might therefore also be responsible for the slight decrease of  $\theta_1$  and  $\theta_2$  above 30 °C. However, the fact that the contribution of  $\beta_\infty$  to the anisotropy decay increases above 30 °C demonstrates that the effect of resonance energy transfer on depolarization is limited.

For FITC-N/Ps, the data could also be fitted using the same uncorrelated or nonassociative model (e.g., three fluorescence lifetimes in combination with two rotational correlation times). We observed rotational correlation times at relatively low temperatures that are close to the corresponding ones of the highly

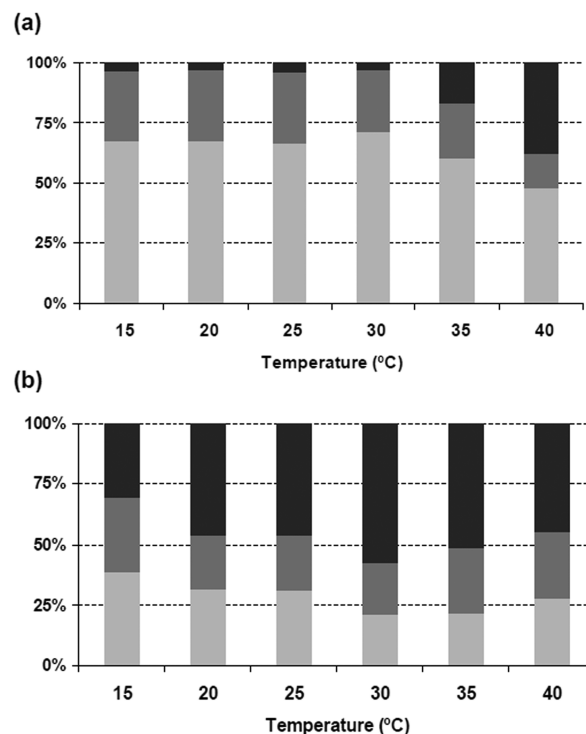


**Figure 5.** Contribution (%) of rotational correlation times and residual anisotropy to the fluorescence anisotropy decay for FITC-N (a) and FITC-N/Ps (b) as a function of temperature in PBS, relative to the total sum:  $\beta_1 + \beta_2 + \beta_\infty$  (which equals the initial anisotropy,  $r_0$ , at time zero). The contributions of the relatively short rotational correlation time,  $\theta_1$  (light gray), the relatively long rotational correlation time,  $\theta_2$  (dark gray), as well as the residual anisotropy,  $\beta_\infty$  (black), are represented.

diluted reference FITC-N. FITC-N/Ps has already a high  $\beta_\infty$  (0.11) at 15 °C (Figure 5b, Table 2). This may originate from reduced rotational motion of the dye possibly caused by interactions of the FITC-labeled PNIPAAm with PEG, which is present on the inner surface of Ps. This is supported by the work of Polozova and Winnik,<sup>29</sup> stating that amide groups of PNIPAAm may form hydrogen bonds with ethylene oxide units of PEG. At 30 °C,  $\theta_2$  for FITC-N/Ps significantly increased as compared to  $\theta_2$  at relatively low temperatures, which is in contrast with the observed decrease of these parameters with increasing temperature for dilute FITC-N samples. These findings can be explained by an increase of the interchain aggregation of PNIPAAm with increasing temperature possibly in concert with phase separation and hydrogel formation. Note that again resonance energy transfer must be limited because aggregation would lead to a decrease of  $\theta_2$ . However, an initial increase of  $\beta_\infty$  from 0.11 to 0.21 upon raising the temperature of FITC-N/Ps from 15 to 25 °C is followed by a gradual decrease of  $\beta_\infty$  to 0.15 upon further increase of temperature. The increased dynamics at relatively high temperature can be explained by the fact that FITC is highly negatively charged at pH 7.4<sup>16</sup> and may therefore be expelled from the relatively apolar hydrogel, forming globular structures, and by that it may reside in the more polar, less viscous aqueous phase. When the phase transition occurs, the gel phase has a volume of 10–20% of the original volume, and the remainder forms an aqueous phase (syneresis).<sup>30–32</sup> A PNIPAAm polymer used in the study formed a macroscopic hydrogel in PBS (5 wt %) above the LCST.

The volume of the hydrogel was about 10% of the original solution in volume (data not shown).

## CONCLUSIONS

PNIPAAm was labeled with FITC (FITC-N) and incorporated into polymersomes. The time-resolved fluorescence as well as the time-resolved fluorescence anisotropy of FITC-N in PBS in polymersomes were monitored as a function of temperature and compared to the results for FITC-N dissolved in PBS at pH 7.4. The results of the FL and TRFA measurements indicate that with increasing temperature PNIPAAm incorporated in Ps undergoes a coil to globule transition followed by intermolecular aggregation and possibly phase separation followed by hydrogel formation. In a future study, it would be interesting to use also other types of fluorescently labeled hydrogels to investigate the effect of the physicochemical properties of the hydrogels on the time-resolved fluorescence and time-resolved fluorescence anisotropy.

## AUTHOR INFORMATION

### Corresponding Author

\*Tel.: +31 53 4892976/4892968. Fax: +31 53 4892155. E-mail: j.feijen@tnw.utwente.nl.

## REFERENCES

- (1) Discher, B. M.; Hammer, D. A.; Bates, F. S.; Discher, D. E. *Curr. Opin. Colloid Interface Sci.* **2000**, *5*, 125.
- (2) Lee, J. C. M.; Bermudez, H.; Discher, B. M.; Sheehan, M. A.; Won, Y. Y.; Bates, F. S.; Discher, D. E. *Biotechnol. Bioeng.* **2001**, *73*, 135.
- (3) Photos, P. J.; Bacakova, L.; Discher, B.; Bates, F. S.; Discher, D. E. *J. Controlled Release* **2003**, *90*, 323.
- (4) Bermudez, H.; Brannan, A. K.; Hammer, D. A.; Bates, F. S.; Discher, D. E. *Macromolecules* **2002**, *35*, 8203.
- (5) Meng, F. H.; Zhong, Z. Y.; Feijen, J. *Biomacromolecules* **2009**, *10*, 197.
- (6) Furryk, S.; Zhang, Y. J.; Ortiz-Acosta, D.; Cremer, P. S.; Bergbreiter, D. E. *J. Polym. Sci., Part A: Polym. Chem.* **2006**, *44*, 1492.
- (7) Jeong, B.; Kim, S. W.; Bae, Y. H. *Adv. Drug Delivery Rev.* **2002**, *54*, 37.
- (8) Lee, J. S.; Zhou, W.; Meng, F. H.; Zhang, D. W.; Otto, C.; Feijen, J. *J. Controlled Release* **2010**, *146*, 400.
- (9) Jesorka, A.; Markstrom, M.; Karlsson, M.; Orwar, O. *J. Phys. Chem. B* **2005**, *109*, 14759.
- (10) Koehorst, R. B. M.; Spruijt, R. B.; Hemminga, M. A. *Biophys. J.* **2008**, *94*, 3945.
- (11) Vanparidon, P. A.; Shute, J. K.; Wirtz, K. W. A.; Visser, A. J. W. G. *Eur. Biophys. J. Biophys. Lett.* **1988**, *16*, 53.
- (12) Rangarajan, B.; Coons, L. S.; Scranton, A. B. *Biomaterials* **1996**, *17*, 649.
- (13) Flint, N. J.; Gardebrecht, S.; Swanson, L. *J. Fluoresc.* **1998**, *8*, 343.
- (14) Eleftheriou, N. M.; Brennan, J. D. *J. Sol-Gel Sci. Technol.* **2009**, *50*, 184.
- (15) Pastor, I.; Ferrer, M. L.; Lillo, M. P.; Gomez, J.; Mateo, C. R. *J. Phys. Chem. B* **2007**, *111*, 11603.
- (16) Sjoback, R.; Nygren, J.; Kubista, M. *Spectrochim. Acta, Part A* **1995**, *51*, L7.
- (17) O'Connor, D. V.; Phillips, D. *Time Correlated Single Photon Counting*; Academic Press: London, 1984.
- (18) van Oort, B.; Ereemeeva, E. V.; Koehorst, R. B.; Laptienok, S. P.; van Amerongen, H.; van Berkel, W. J.; Malikova, N. P.; Markova, S. V.; Vysotski, E. S.; Visser, A. J.; Lee, J. *Biochemistry* **2009**, *48*, 10486.
- (19) Visser, N. V.; Westphal, A. H.; van Hoek, A.; van Mierlo, C. P. M.; Visser, A.; van Amerongen, H. *Biophys. J.* **2008**, *95*, 2462.
- (20) Digris, A. V.; Skakoun, V. V.; Novikov, E. G.; van Hoek, A.; Claiborne, A.; Visser, A. J. W. G. *Eur. Biophys. J. Biophys. Lett.* **1999**, *28*, 526.
- (21) van den Berg, P. A. W.; van Hoek, A.; Visser, A. J. W. G. *Biophys. J.* **2004**, *87*, 2577.
- (22) van Hoek, A.; Vos, K.; Visser, A. J. W. G. *IEEE J. Quantum Electron.* **1987**, *QE-23*, 1812.
- (23) Lakowicz, R. J. *Principles of Fluorescence Spectroscopy*, 3rd ed.; Springer: New York, 2006.
- (24) van Oort, B.; Amunts, A.; Borst, J. W.; van Hoek, A.; Nelson, N.; van Amerongen, H.; Croce, R. *Biophys. J.* **2008**, *95*, 5851.
- (25) Duan, C. K.; Meijerink, A.; Reeves, R. J.; Reid, M. F. *J. Alloys Compd.* **2006**, *408*, 784.
- (26) Yang, J.; Roller, R. S.; Winnik, M. A. *J. Phys. Chem. B* **2006**, *110*, 11739.
- (27) Rangelowa, S.; Kulak, L.; Gryczyński, I.; Sakar, P.; Bojarski, P. *Chem. Phys. Lett.* **2008**, *452*, 105.
- (28) Wu, C.; Zhou, S. Q. *Macromolecules* **1995**, *28*, 8381.
- (29) Polozova, A.; Winnik, F. M. *Langmuir* **1999**, *15*, 4222.
- (30) Suzuki, Y.; Tomonaga, K.; Kumazaki, M.; Nishio, I. *Polym. Gels Networks* **1996**, *4*, 129.
- (31) Ruel-Gariepy, E.; Leroux, J. C. *Eur. J. Pharm. Biopharm.* **2004**, *58*, 409.
- (32) Ito, K.; Ujihira, Y.; Yamashita, T.; Horie, K. *Polymer* **1999**, *40*, 4315.